

Towards a systematic design of isotropic bulk magnetic metamaterials using the cubic point groups of symmetry

J. D. Baena,^{*} L. Jelinek,[†] and R. Marqués[‡]

Departamento de Electrónica y Electromagnetismo, Universidad de Sevilla, Avenida Reina Mercedes s/n, 41012 Sevilla, Spain

(Received 8 May 2007; revised manuscript received 27 September 2007; published 17 December 2007)

In this paper, a systematic approach to the design of bulk isotropic magnetic metamaterials is presented. The roles of the symmetries of both the constitutive element and the lattice are analyzed. For this purpose, it is assumed that the metamaterial is composed of cubic split ring resonators (SRRs) arranged in a cubic lattice. The minimum symmetries needed to ensure an isotropic behavior are analyzed, and some particular configurations are proposed. Besides, an equivalent circuit model is proposed for the considered cubic SRRs. Experiments are carried out in order to validate the proposed theory. We hope that this analysis will pave the way to the design of bulk metamaterials with strong isotropic magnetic response, including negative permeability and left-handed metamaterials.

DOI: 10.1103/PhysRevB.76.245115

PACS number(s): 42.70.Qs, 41.20.Jb, 42.25.Bs

I. INTRODUCTION

Metamaterials are artificial media exhibiting exotic electromagnetic properties not previously found in nature. Among them, media showing simultaneously negative electric permittivity and magnetic permeability in some frequency range, or “left-handed” metamaterials, are of particular interest. The striking properties of left-handed metamaterials, including backward-wave propagation, negative refraction, and inverse Cerenkov and Doppler effects were first reported by Veselago¹ in 1968. However, the realistic implementations of left-handed metamaterials came several decades later, as a combination of split ring resonators (SRRs) and metallic wires.² SRRs are small planar resonators exhibiting a strong magnetic response, which were proposed in 1999 by Pendry *et al.*³ as suitable “atoms” for the development of negative magnetic permeability metamaterials. One year later, Smith *et al.* demonstrated the possibility of making up a left-handed medium by periodically combining metallic wires—which provide an effective negative permittivity at microwaves⁴—and SRRs.² In subsequent works, other SRR designs were proposed,^{5–8} in order to reduce electrical size and/or cancel the bianisotropic behavior of the original Pendry’s design. However, all the aforementioned implementations of negative permeability and left-handed metamaterials are highly anisotropic—or even bianisotropic⁵—providing only a uniaxial resonant magnetization, while isotropy is needed for many interesting applications of metamaterials, as, for instance, the “perfect lens” proposed by Pendry.⁹

The aforementioned implementations are, in fact, a combination of two separate systems, one providing the negative magnetic permeability (the SRR system) and the other providing the negative electric permittivity (the wire system). How both subsystems can be combined in order to obtain a new system, whose electromagnetic properties were mainly the superposition of the magnetic and the electric properties of each subsystem, is an interesting and controversial issue^{10,11} that is, however, beyond the scope of this paper. In what follows, we will assume that it is possible to find some combination of two isotropic subsystems, one made of me-

talic wires (or other elements providing a negative electric permittivity) and the other made of SRRs, whose superposition gives a left-handed metamaterial, and will focus our attention on the design of isotropic systems of SRRs. Actually, since isotropic media with negative magnetic permeability are not found in nature, an isotropic system of SRRs providing such property in some frequency range will be an interesting metamaterial by itself. These metamaterials could provide the dual of negative electric permittivity media, with similar applications (in imaging,⁹ for instance). They would be also of interest for magnetic shielding and other practical applications.

A first attempt to design an isotropic magnetic metamaterial was carried out by Gay-Balmaz and Martin,¹² who designed a spherical magnetic resonator—formed by two SRRs crossed in right angle—which is isotropic in two dimensions. This result was later generalized in Ref. 13, where a fully isotropic spherical magnetic resonator was proposed. However, from a practical standpoint, it is usually easier to work with cubic designs. A first attempt on such direction was made by Simovski and co-workers in Refs. 14–16, where cubic arrangements of planar SRRs and omega particles were proposed [see Figs. 1(a) and 1(b)]. If only the magnetic and/or electric dipole representations of the SRRs and/or omega particles are considered, these arrangements are invariant under cubic symmetries. However, it has been shown^{13,17} that this invariance is not enough to guarantee an isotropic behavior since couplings between the planar resonators forming the cubic arrangement can give rise to an anisotropic behavior, even if its dipole representations suggest an isotropic design. The first isotropic metamaterial design fully invariant under the whole group of symmetry of the cube was proposed and simulated in Ref. 18. It is formed by volumetric square SRRs with four gaps, in order to provide 90° rotation symmetries about any of the cube axes. However, this design is unfortunately very difficult to implement in practice because it cannot be manufactured by using standard photoetching techniques, as previous SRR designs,^{2,3,5–8,13–17} and the gaps of the SRR have to be filled with a high relative permittivity dielectric (about 100). The idea of using spatial symmetries to design isotropic metama-

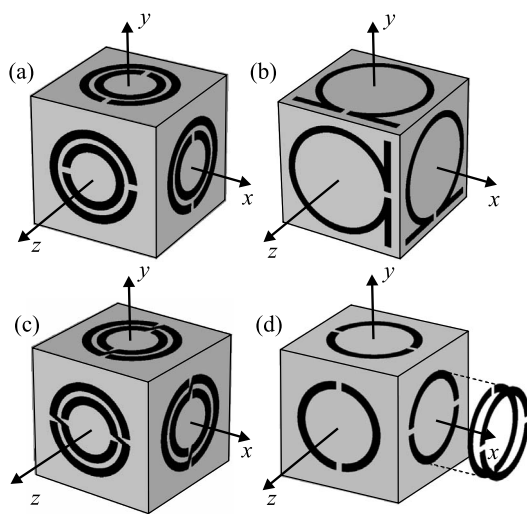


FIG. 1. Cubic constitutive elements for isotropic metamaterial design. Cubes (a) and (b) were studied in Refs. 14–16. Their hidden faces are arranged in such a way that the cube satisfies the central symmetry to avoid magnetoelectric coupling. Cubes (c) and (d) were proposed in Ref. 13 as truly three-dimensional (3D) isotropic cubic resonators.

terials was further developed in Refs. 13, 17, and 19 leading to the structures depicted in Figs. 1(c) and 1(d).

A second group of attempts to design isotropic metamaterials is developed in Ref. 20 and 21. In these works, lattices of dielectric and/or paramagnetic spheres with very high refractive index are proposed. If the refractive index of the spheres is high enough, the internal wavelength becomes small with regard to the macroscopic wavelength, and Mie resonances of the spheres can be used to produce the negative effective permittivity and/or permeability. Since the metamaterial “atoms” are spheres, the isotropy is ensured by simply placing them in a cubic lattice. However, practical difficulties to implement such proposals are not easy to overcome. First of all, lossless media with the very high refractive index needed for the spheres are difficult to obtain. Secondly, the system has a very narrow band.²¹

All the previously reported proposals for isotropic magnetic metamaterial design use a “crystal-like” approach. That is, they are based on the homogenization of a system of magnetic resonators which, according to causality laws, exhibit a strong diamagnetic response above resonance. There is, however, another approach widely used in the microwave community which is based on the transmission line analogy to effective media. Initially proposed for two-dimensional metamaterial design,²² it was recently generalized to three-dimensional isotropic structures.^{23–26} The main advantage of this approach is its broadband operation, since no resonators are necessary for the design. However, it also presents disadvantages with regard to crystal-like approaches. The transmission line approach to metamaterials does not seem to be applicable beyond the microwave range, whereas a significant magnetic response of the SRR has been shown in the terahertz range and beyond.^{27,28} In addition, the coupling to free space of the reported transmission line metamaterials seems to be difficult and sometimes needs an additional spe-

cific interface (e.g., an antenna array²⁵), whereas this coupling is direct in crystal-like metamaterials.

Finally, regarding isotropic left-handed metamaterial design, it should be mentioned that some recent proposals based on random arrangements of chiral particles^{29,30} have the advantage of providing simultaneously both electric and magnetic negative polarizabilities. This approach can be straightforwardly extended to the design of SRR magnetic metamaterials, by simply considering random arrangements of such elements. There is, however, a major difficulty with this approach: the constitutive elements in a random composite have to be very small in comparison with the macroscopic wavelength to show a true statistical behavior, but it is not easy to design a SRR much smaller than one-tenth of the wavelength. Due to this fact, periodic arrangements will be considered in what follows.

The main aim of this paper is to present a systematic approach to the design of metamaterial structures based on periodic arrangements of SRRs. The first section is focused on the spatial symmetries which are necessary to ensure an isotropic behavior in the metamaterial. Cubic arrangements of SRRs placed on cubic lattices are considered, and the minimum symmetry requirements for both the individual resonators and the lattices are investigated. The second section is devoted to a deeper analysis of the isotropic cubic SRRs forming the basis of the crystal structure. In the third section, an equivalent circuit model for such cubic SRRs is developed and applied to some specific examples. The fourth section is focused on the experimental verification of the analysis developed in the previous ones. Finally, the main conclusions of the work are presented.

II. ROLE OF CUBIC SYMMETRIES

Let us assume that constitutive elements and the unit cell of the material are much smaller than the operating wavelength. In such a case, the interaction of electromagnetic field with the material is described by means of constitutive relations. Besides, the material is supposed to be linear, so the most general way to express those relations between electromagnetic intensities and electromagnetic flux densities is³¹

$$\mathbf{D} = \boldsymbol{\epsilon} \cdot \mathbf{E} + \boldsymbol{\xi} \cdot \mathbf{H},$$

$$\mathbf{B} = \boldsymbol{\zeta} \cdot \mathbf{E} + \boldsymbol{\mu} \cdot \mathbf{H}, \quad (1)$$

where $\boldsymbol{\epsilon}$, $\boldsymbol{\mu}$ are second rank constitutive tensors and $\boldsymbol{\xi}$, $\boldsymbol{\zeta}$ are second rank constitutive pseudotensors. In order to get a macroscopic isotropic behavior, all constitutive tensors and pseudotensors $\boldsymbol{\epsilon}$, $\boldsymbol{\mu}$, $\boldsymbol{\xi}$, and $\boldsymbol{\zeta}$ must become scalars or pseudoscalars.

Let us now address the problem of forcing the tensors (or pseudotensors) in Eq. (1) to be scalars (or pseudoscalars) for the specific case of a periodic structure. It is well known^{32,33} that there are 32 symmetry point groups for periodic crystals which can be classified in 7 crystallographic systems. It is also known that the cubic system is the only one that forces any second rank tensor (or pseudotensor) to be a scalar (or a pseudoscalar).³³ Since any material satisfying the linear constitutive relations [Eq. (1)] and being invariant under the cu-

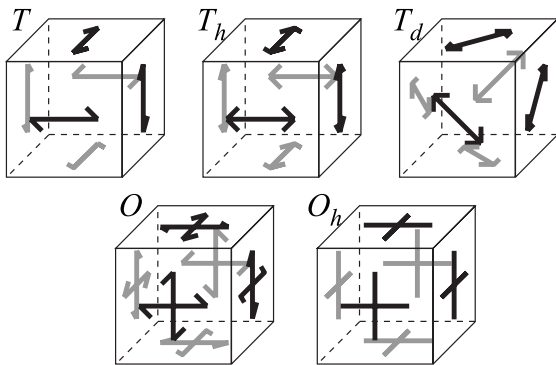


FIG. 2. Objects with the symmetries of the five cubic point groups.

bic symmetries exhibits an isotropic macroscopic behavior, this section will be focused on the analysis of such cubic symmetries. It is clear that any structure invariant under all the symmetry transformations of the cube must be isotropic, as already proposed by Koschny *et al.*¹⁸ Furthermore, the full symmetry group of the cube contains four different subgroups also belonging to the cubic system and, thus, providing an isotropic macroscopic behavior. Since a less symmetric design is subjected to less structural constraints, it may be guessed that using these subgroups—instead of the whole symmetry group of the cube—may have practical advantages. Keeping this in mind, we will first give a short overview on the five cubic point groups. Next, we shall connect these point groups with some real structures made of planar resonators commonly used in metamaterials. This will be done in two parts: the study of the symmetries of the constitutive element, or the *basis*, and the analysis of the suitable periodic arrangements, or the *lattice*. At the end of the section some practical isotropic structures will be specifically analyzed.

A. Cubic point groups

The five cubic point groups are schematically represented in Fig. 2. Following Schöenflies' notation and ordering by degree of symmetry, these groups and their generators are as follows:

- (1) $T = \langle \{1, \mathbf{4}_x, \mathbf{4}_y, \mathbf{4}_z\} \rangle$ = proper rotations of the regular tetrahedron (12 operations);
- (2) $T_h = \langle \{1, -1, \mathbf{4}_x, \mathbf{4}_y, \mathbf{4}_z\} \rangle = T$ expanded by the inversion (24 operations);
- (3) $T_d = \langle \{1, -2_x, \mathbf{4}_x, \mathbf{4}_y, \mathbf{4}_z\} \rangle$ = proper and improper rotations of the regular tetrahedron (24 operations);
- (4) $O = \langle \{1, \mathbf{4}_x, \mathbf{4}_y\} \rangle$ = proper rotations of the cube (24 operations);
- (5) $O_h = \langle \{1, -1, \mathbf{4}_x, \mathbf{4}_y\} \rangle$ = full symmetry group of the cube (48 operations).

We have used a widely used notation for symmetry transformations, $\mathbf{1}$ being the identity operator, -1 the inversion, \mathbf{n}_p an n -fold rotation axis about the p axis, and $-\mathbf{n}_p$ the n -fold axis about the p axis followed by the inversion. For example, the operator -2_x is the rotation through 180° about the x axis followed by the inversion.

B. Cubic basis

In order to simplify the problem, the symmetries can be separately imposed on the basis and the lattice of the structure. For the sake of simple fabrication, we will assume that the basis is formed by six planar resonators placed over the faces of an inert rigid cube, as in Fig. 1. If the crystal was diluted enough, then the coupling between two neighboring cubes would be much weaker than the coupling between the six SRRs of the same cube and thus each cube could be seen as a single cubic resonator (CR) electromagnetically coupled to others. Such consideration implies that the interaction between the CRs forming the material can be described by dipole-dipole interactions, higher order multipole interactions being negligible. In such approximation, all the CRs are properly described by second rank polarizability tensors connecting the external field, \mathbf{E}^{ext} and \mathbf{B}^{ext} , with the dipolar moments, \mathbf{p} and \mathbf{m} , induced in the CRs,^{31,34}

$$\mathbf{p} = \boldsymbol{\alpha}_{ee} \cdot \mathbf{E}^{ext} + \boldsymbol{\alpha}_{em} \cdot \mathbf{B}^{ext},$$

$$\mathbf{m} = \boldsymbol{\alpha}_{mm} \cdot \mathbf{B}^{ext} - \boldsymbol{\alpha}_{em}^t \cdot \mathbf{E}^{ext}, \quad (2)$$

where $\boldsymbol{\alpha}_{ee}$, $\boldsymbol{\alpha}_{mm}$, and $\boldsymbol{\alpha}_{em}$ are the electric, magnetic, and magnetoelectric polarizability tensors, and the superscript t means transpose operation. The constitutive tensors in Eq. (1) can be derived from these polarizabilities and from the lattice structure by applying a homogenization technique.

In what follows, different kinds of CRs will be named by its cubic group symmetry followed by the acronym CR (group-CR). In order to design an isotropic CR, we have to find suitable planar resonators and place them correctly over the cube so as to fulfill the necessary symmetries. Obviously, the planar resonators have to be invariant under certain symmetry transformations of the square. To classify all different possibilities, a list of the symmetry subgroups of the square is shown in Table I, as well as their geometrical representations, and some examples of planar resonators commonly used in metamaterial design and obeying these symmetries. This table also provides a systematic terminology for planar resonators by using the symbol of the symmetry group followed by the term SRR (group-SRR). In what follows, we will use the term SRR in a general sense covering any type of geometry derived from the SRR and the omega particle.

By direct inspection on Fig. 2, it can be seen that any of the five cubic point groups contains three twofold rotation axes (180° rotations) parallel to the edges of the cube. Thus, only resonators belonging to the last five rows of Table I are appropriate for designing isotropic CRs. At this point, it may be worth mentioning that Pendry's SRRs³ as well as Omega particles³⁵ are not appropriate for such purpose because they correspond to the C_1 -SRR and D_1 -SRR topologies. In summary, in order to get an isotropic CR, we have to choose six identical SRRs pertaining to the classes C_2 , D_2 , C_4 , or D_4 -SRR and arrange them according to one of the cubic point groups T , T_d , T_h , O , or O_h shown in Fig. 2.

Although all five cubic point groups mentioned above are equally useful to achieve isotropic CRs, a specific choice may strongly affect the properties of an isotropic metamaterial. For instance, using isotropic CRs of low symmetry may

TABLE I. Classification of SRR types based on the symmetry subgroups of the square. The second column shows Schöenflies' notation and the generator of groups. The symbols of transformations are **1**=identity; **4**=90° rotation; **2**=180° rotation; **-4**=-90° rotation; \mathbf{m}_x , \mathbf{m}_y =line reflections respect to the x and y axes, respectively; $\mathbf{m}_{x,y}$, $\mathbf{m}_{x,-y}$ =line reflections respect to both diagonals of the square. Each group is schematically represented by the objects in the second column which can be replaced by the planar resonators shown in the third column.

SRR types	Symmetry subgroups of the square	Geometrical representation	Examples of resonators
C_1 -SRR	$C_1 = \{\mathbf{1}\}$		
D_1 -SRR	$D_{1x} = \{\mathbf{1}, \mathbf{m}_x\}$		
	$D_{1y} = \{\mathbf{1}, \mathbf{m}_y\}$		
	$D_{1,x,y} = \{\mathbf{1}, \mathbf{m}_{x,y}\}$		
	$D_{1,x,-y} = \{\mathbf{1}, \mathbf{m}_{x,-y}\}$		
C_2 -SRR	$C_2 = \{\mathbf{1}, \mathbf{2}\}$		
D_2 -SRR	$D_{2x} = D_{2y} = \{\mathbf{1}, \mathbf{m}_x, \mathbf{m}_y, \mathbf{2}\}$		
	$D_{2xy} = D_{2x,-y} = \{\mathbf{1}, \mathbf{m}_{x,y}, \mathbf{m}_{x,-y}, \mathbf{2}\}$		
C_4 -SRR	$C_4 = \{\mathbf{1}, \mathbf{4}, \mathbf{2}, \mathbf{-4}\}$		
D_4 -SRR	$D_4 = \{\mathbf{1}, \mathbf{4}, \mathbf{2}, \mathbf{-4}, \mathbf{m}_x, \mathbf{m}_y, \mathbf{m}_{x,y}, \mathbf{m}_{x,-y}\}$		

be quite advantageous since the electrical size of the CRs can be made smaller. This fact can be justified in terms of the LC circuit models for the SRRs^{5–8} because the effective capacitances of low symmetry SRRs are usually higher than those of high symmetry SRRs,⁸ thus providing a smaller resonance frequency. Following these considerations, the best choice of basis would be a T -CR made of six planar resonators of the C_2 -SRR type. A good candidate among all possibilities is the cube shown in Fig. 1(c) made of six nonbianisotropic SRRs (NB-SRRs),^{8,36} a configuration already proposed in Refs. 13 and 17. Furthermore, it was shown in Ref. 13 that this configuration shows a bi-isotropic behavior, due to the lack of inversion symmetry of the cubic arrangement. However, sometimes, an effective isotropic medium without biaxiality ($\xi, \zeta=0$) is desired. Since ξ and ζ are pseudotensors, the invariance of the CR under inversion is required in order to avoid such property. In this case, the lowest symmetry group is the T_h group. A CR invariant under the last group of symmetry can be made by using planar resonators of the D_2 -SRR type as, for instance, the symmetric SRR³⁷ or the modified double-slit broadside coupled SSR (BC-SRR) shown in Fig. 1(d).¹³ However, as will be shown in the following, such symmetry requirements can be relaxed if the lattice symmetries are properly chosen.

C. Cubic lattices

Above findings give precise instructions for choosing suitable geometries for isotropic metamaterial constitutive elements. The next step is to create an isotropic metamaterial with these elements. The cubic shape of the considered constitutive elements suggests that the best periodical arrangements are the simple cubic (sc), body centered cubic (bcc), and face centered cubic (fcc) lattices shown in Fig. 3. All these lattices obey the full symmetry group of the cube, O_h . Therefore, the whole metamaterial (lattice plus basis) retains the cubic point group symmetries and the macroscopic isotropic behavior.

Although all previously mentioned lattices can provide isotropic metamaterials, it is convenient to look deeply into the possible structures because some particular choices may offer interesting advantages. Regarding Fig. 3, a is the edge size of the CR and b is the edge size of the cubic unit cell. In order to describe CR interactions as dipole-dipole interactions, b must be chosen much larger than a , so that the metamaterial properties can be deduced from Eq. (2) and the appropriate homogenization procedure. However, usually, we are also interested in a high density of dipoles in order to get a strong electromagnetic response. Therefore, b should

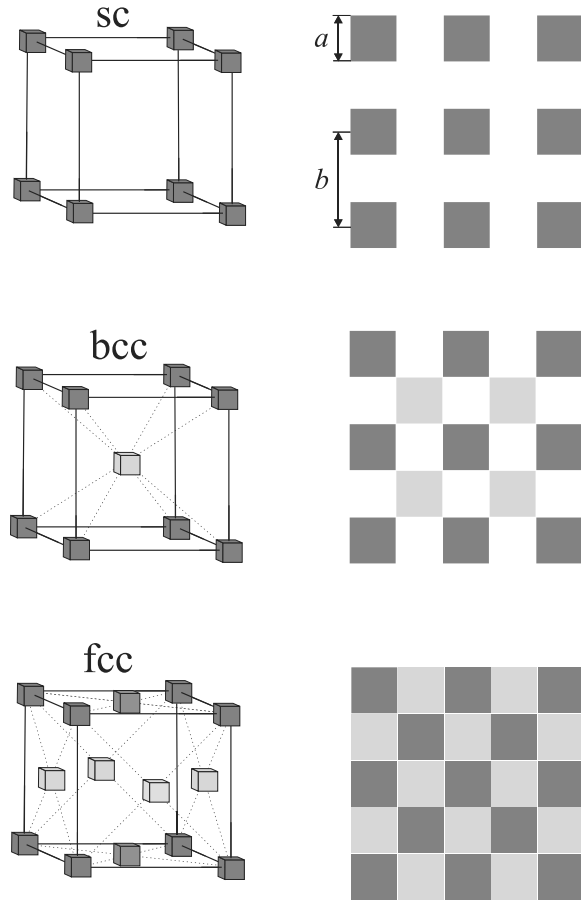


FIG. 3. Cubic Bravais' lattices. Their top views are also depicted for the particular case of $b=2a$. Black and gray small cubes represent cubic resonators on successive planes.

be as small as possible. However, decreasing b may lead to a failure of the aforementioned homogenization procedure. However, in any case, the combination of a basis and a lattice with the appropriate symmetries will provide an isotropic metamaterial, regardless of the homogenization procedure. Finally, there are some practical limitations to the values that a and b can reach as, for instance, the obvious inequality $b \geq a$, derived from the fact that CRs are supposed to be impenetrable.

Additional limitations appear for each specific structure. In the case of a sc lattice with T -, T_d -, or O -CRs, the lack of inversion symmetry implies that opposite sides of a CR are not oriented in the same way. Thus, the constrain $b > a$ is necessary in order to avoid a mutual short circuit between the SRRs of neighboring CRs. To allow the minimum distance $b=a$, the noncentrosymmetric CRs in the sc lattice must be replaced by T_h - or O_h -CRs, so that the SRRs on contacting sides of neighboring CRs exactly overlap. In the case of a bcc lattice, the contact between corners implies that the inequality $b \geq a$ must be fulfilled for any type of CR. Finally, for the fcc lattice, the contact between edges of neighboring CRs establishes the harder condition $b \geq 2a$.

The particular case of an fcc lattice with the minimum cell size, $b=2a$, deserves a specific analysis. When T_h - or O_h -CRs are used as the basis of the fcc lattice, the structure

turns into an sc lattice with the highest possible compactness, i.e., $b=a$, because the *holes* between each eight neighboring CRs have the same shape as the CRs forming the basis. The case of an fcc lattice with a T -, T_d -, or O -CR basis is even more special and interesting because each hole exactly corresponds with the inversion of the CR of the basis. Therefore, although the basis of the structure is not invariant under inversion, the fcc structure is brought into coincidence with itself by inversion centered at the center of a CR, followed by a translation of length a through any of the cube axes. Since the wavelength of the signal illuminating the structure is supposed to be much larger than a , the system can be considered as macroscopically invariant under inversion and, therefore, any bi-isotropic behavior must disappear. Thus, we conclude that a very interesting choice in order to obtain an isotropic metamaterial is the fcc lattice with $b=2a$ and with a basis formed by T -CRs [example in Fig. 1(c)] because of its high compactness, non-bi-isotropic macroscopic behavior, and low degree of symmetry. It is worth recalling here that T -CRs have the lowest symmetry among all the possibilities shown in Fig. 2, which helps to reduce the electrical size of the unit cell, as explained above.

III. RESONANCES AND POLARIZABILITIES OF CUBIC RESONATORS

Until now, only the symmetry of CRs and cubic lattices useful for isotropic periodic metamaterials were analyzed. However, in order to have a complete characterization of the metamaterial, polarizabilities and couplings between individual SRRs must be considered. In dilute crystals, the approach of weak coupling between CRs, but strong coupling between the SRRs of each CR, is valid. Then, the metamaterial characterization involves two separate problems: obtaining the polarizability tensors in Eq. (2) for a single CR and applying the appropriate homogenization procedure to obtain the constitutive parameters for the whole structure. For dense packages, the aforementioned approach is not valid since couplings between SRRs of different CRs can be stronger than SRR couplings inside each individual CR. However, even in these cases, the analysis of the isolated CR resonances and polarizabilities still provides useful information on the behavior of the metamaterial. For instance, it allows to elucidate if the coupling between SRRs in a practical low symmetry CR can be neglected or not. In case they could be neglected, all the analysis in Sec. II B would become irrelevant because the SRRs could be substituted by its equivalent dipoles (as it was assumed in Refs. 14–16), without more considerations on the SRR structure. Therefore, the analysis in this section is necessary in order to justify the practical relevance of the analysis developed in Sec. II. Further, in Sec. IV, an experimental validation of this analysis will be provided.

Let us assume that the CR size is much smaller than the operating wavelength. Thus, an RLC circuit model is valid for describing the behavior of single Pendry's SRRs,³ as well as for any type of modified SRRs^{5–8} or omega particles.³⁸ Furthermore, if the resonators are not too close (so that the interaction energies are small with regard to the self-energy

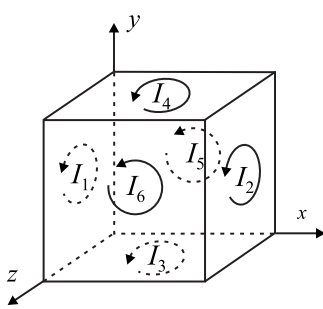


FIG. 4. Definition of the sign of currents in the circuit model for a 3D cubic magnetic resonator.

of each SRR), then the CR can be considered as six *RLC* circuits coupled through mutual impedances. The positive directions of the electric currents on each loop are arbitrarily defined in Fig. 4. The relation between currents and electromotive forces exciting the CR can be written as

$$\mathbf{Z} \cdot \mathbf{I} = \mathbf{F}, \quad (3)$$

where \mathbf{Z} is a 6×6 square impedance matrix, \mathbf{I} is a column matrix whose i th component is the current flowing over the i th SRR, and \mathbf{F} is a column matrix whose i th component is the external electromotive force acting on the i th SRR. The diagonal components of the impedance matrix are the self-impedances of each SRR, i.e., $Z_{ii}=R+j\omega L+1/(j\omega C)$, with R , L , and C being the resistance, self-inductance, and self-capacitance of a single SRR.⁸ The nondiagonal components Z_{ij} are the mutual impedances between the i th and j th SRRs. From the reciprocity theorem,³⁹ we know that the impedance matrix must be symmetric, i.e., $Z_{ij}=Z_{ji}$. This reduces the number of independent elements of \mathbf{Z} to 21. This number can be further reduced by applying the geometrical symmetries of the CR, as shown in the next paragraph.

The application of any symmetry operation changes the components of \mathbf{I} according to the rule $\mathbf{I}'=\mathbf{S} \cdot \mathbf{I}$, where \mathbf{S} is the corresponding operator of symmetry. It is well known that any symmetry operation \mathbf{S} of the cubic point groups can be expressed as some combination of the three orthogonal four-fold rotations and the inversion, whose matrix representations, in the six-dimensional space defined by \mathbf{I} , are

$$\begin{aligned} \mathbf{4}_x &= \left[\begin{array}{c|cc|c} 1 & 0 & 0 & 0 \\ 0 & 1 & 0 & 0 \\ \hline 0 & 0 & 0 & 0 \\ & 0 & -1 & 0 \\ & -1 & 0 & 0 \end{array} \right], \\ \mathbf{4}_y &= \left[\begin{array}{c|cc|c} 0 & 0 & 1 & 0 \\ 0 & 1 & 0 & 0 \\ \hline 0 & 0 & 0 & 0 \\ & 0 & 1 & 0 \\ & 1 & 0 & 0 \\ & 0 & 0 & 0 \end{array} \right], \end{aligned}$$

$$\begin{aligned} \mathbf{4}_z &= \left[\begin{array}{c|cc|c} 0 & 0 & -1 & 0 \\ -1 & 0 & 0 & 0 \\ \hline 1 & 0 & 0 & 0 \\ 0 & 1 & 0 & 0 \\ \hline 0 & 0 & 1 & 0 \\ 0 & 0 & 0 & 1 \end{array} \right], \\ -\mathbf{1} &= \left[\begin{array}{c|cc|c} 0 & 1 & 0 & 0 \\ 1 & 0 & 0 & 0 \\ \hline 0 & 0 & 1 & 0 \\ & 1 & 0 & 0 \\ & 0 & 0 & 0 \\ & 0 & 0 & 1 \end{array} \right]. \end{aligned} \quad (4)$$

They are unitary matrices with the well known property $\mathbf{S}^{-1}=\mathbf{S}^t$. It can be straightforwardly demonstrated that \mathbf{F} follows the same rule of transformation: $\mathbf{F}'=\mathbf{S} \cdot \mathbf{F}$. Therefore, both \mathbf{I} and \mathbf{F} can be considered as vectors. In what follows, \mathbf{I} and \mathbf{F} will be called the “current” and the “excitation” vectors, respectively. Therefore, the impedance matrix \mathbf{Z} is a second rank tensor, following the transformation rule $\mathbf{Z}'=\mathbf{S} \cdot \mathbf{Z} \cdot \mathbf{S}^t$. If the CR remains invariant by the transformation \mathbf{S} , then

$$\mathbf{Z} = \mathbf{S} \cdot \mathbf{Z} \cdot \mathbf{S}^t. \quad (5)$$

This equation gives some relations between the components of \mathbf{Z} , which can reduce the number of independent components of \mathbf{Z} .

Although the current vector \mathbf{I} can be directly solved by multiplying both sides of Eq. (3) by \mathbf{Z}^{-1} , in order to identify the different resonances of the CR, it is convenient to expand the solution in terms of the eigenvectors of \mathbf{Z} . The eigenvalue problem corresponding to Eq. (3) is

$$\mathbf{Z} \cdot \mathbf{v}_i = z_i \mathbf{v}_i, \quad (6)$$

where z_i are the eigenvalues, \mathbf{v}_i the eigenvectors, and the index $i=1, \dots, 6$. The impedance matrix \mathbf{Z} can be expanded in a sum of two terms as

$$Z_{ij} = \left(R + j\omega L + \frac{1}{j\omega C} \right) \delta_{ij} + Z_{ij}(1 - \delta_{ij}), \quad (7)$$

where δ_{ij} is Kronecker’s delta. The first term is the self-impedance of a single SRR multiplied by the identity, while the second term is the symmetric matrix of mutual impedances. These mutual impedances are purely imaginary numbers since, in the frame of a quasistatic model, they cannot contain a resistive term. Thus, the second term in Eq. (7) is a purely imaginary symmetrical matrix. Therefore, its eigenvectors can be chosen in such a way that they form a complete and orthogonal basis that diagonalizes this matrix. Furthermore, since the first summand in Eq. (7) is actually a scalar, the eigenvectors of Z_{ij} are actually the same as those of $Z_{ij}(1 - \delta_{ij})$. Therefore, the eigenvectors of \mathbf{Z} can be chosen in such a way that they form an orthogonal basis for the considered six-dimensional space. Thus, the current and ex-

citation vectors can be expanded as a summation of such eigenvectors,

$$\mathbf{I} = \sum_i (\mathbf{I} \cdot \mathbf{v}_i) \mathbf{v}_i, \quad \mathbf{F} = \sum_i (\mathbf{F} \cdot \mathbf{v}_i) \mathbf{v}_i. \quad (8)$$

By substituting both expressions into Eq. (3) and applying Eq. (6), we get

$$\mathbf{I} = \sum_i \frac{\mathbf{F} \cdot \mathbf{v}_i}{z_i} \mathbf{v}_i. \quad (9)$$

Therefore, both \mathbf{F} and \mathbf{I} can be expanded in a set of orthogonal modes having mutually proportional excitation and current vectors.

From Eq. (7), we can also obtain information about the structure of the eigenvalues z_i . These eigenvalues must have the form

$$z_i(\omega) = R + j\omega L + \frac{1}{j\omega C} + z_{c,i}(\omega) = j\omega L \left[1 - \frac{\omega_0^2}{\omega^2} + \frac{R}{j\omega L} + \frac{z_{c,i}(\omega)}{j\omega L} \right], \quad (10)$$

where ω_0 is the resonance frequency of an isolated SRR ($\omega_0^2 = 1/LC$), and $z_{c,i}(\omega)$ the eigenvalues of the second summand in Eq. (7), which are related to the coupling between SRRs. It can be seen in Eq. (9) that the i th mode resonates when its eigenvalue approaches zero ($z_i \approx 0$). Therefore, the frequency of resonance of the i th mode is given by the relation $z_i(\omega_{0,i}) \approx 0$. If losses and couplings between SRRs are not too strong ($R, z_{c,i} \ll j\omega L$), the frequencies of resonance of the CR can be approximated as

$$\omega_{0,i} \approx \omega_0 - \frac{z_{c,i}(\omega_0)}{2jL}. \quad (11)$$

In what follows, we will apply this equivalent circuit model to the determination of the resonances and polarizabilities of two CRs made from two well known SRRs: Pendry's SRR³ and NB-SRR.⁸

A. Analysis of an anisotropic cube

Let us now consider the CR shown in Fig. 1(a), made of Pendry's SRRs. In this section, we are going to get some analytical approximation for its resonances and polarizabilities. Note that the cube possesses inversion symmetry and, thus, magnetoelectric coupling is forbidden, so that $\alpha_{em}=0$ in Eq. (2). It can also be seen by inspection that the considered CR is invariant under the rotation $\mathbf{4}_y \cdot \mathbf{4}_x$. By applying this spatial symmetry, the impedance matrix is reduced to the form

TABLE II. Eigenvalues and a complete set of orthonormal eigenvectors of the impedance matrix [Eq. (12)] corresponding to anisotropic cubic resonators with symmetries $-\mathbf{1}$ and $\mathbf{4}_y \cdot \mathbf{4}_x$, as, for instance, the structures shown in Figs. 1(a) and 1(b).

	Eigenvalues z_i	Eigenvectors \mathbf{v}_i
Even modes (magnetic)	$Z_{11}+Z_{12}-Z_{13}-Z_{14}$	$\frac{1}{2}(-1,-1,1,1,0,0)$ $\frac{1}{2\sqrt{3}}(1,1,1,1,2,2)$
	$Z_{11}+Z_{12}+2Z_{13}+2Z_{14}$	$\frac{1}{\sqrt{6}}(-1,-1,-1,-1,1,1)$
Odd modes (electric)	$Z_{11}-Z_{12}-Z_{13}+Z_{14}$	$\frac{1}{2\sqrt{3}}(1,-1,-2,2,1,-1)$ $\frac{1}{2}(1,-1,0,0,-1,1)$
	$Z_{11}-Z_{12}+2Z_{13}-2Z_{14}$	$\frac{1}{\sqrt{6}}(-1,1,-1,1,-1,1)$

$$\mathbf{Z} = \begin{bmatrix} Z_{11} & Z_{12} & Z_{13} & Z_{14} & -Z_{14} & -Z_{13} \\ Z_{12} & Z_{11} & Z_{14} & Z_{13} & -Z_{13} & -Z_{14} \\ Z_{13} & Z_{14} & Z_{11} & Z_{12} & -Z_{14} & -Z_{13} \\ Z_{14} & Z_{13} & Z_{12} & Z_{11} & -Z_{13} & -Z_{14} \\ -Z_{14} & -Z_{13} & -Z_{14} & -Z_{13} & Z_{11} & Z_{12} \\ -Z_{13} & -Z_{14} & -Z_{13} & -Z_{14} & Z_{12} & Z_{11} \end{bmatrix}, \quad (12)$$

where there are only four independent components. The corresponding eigenvalues and its orthonormal eigenvectors are shown in Table II. It is worth noting that the eigenvectors can be classified in even and odd modes: for even (odd) modes, the currents I_{2n-1} and I_{2n} are parallel (antiparallel).

Once the eigenvalue problem is solved, the next step is to write an explicit expression for the excitation vector \mathbf{F} and introduce this expression in Eq. (9), in order to get the currents over the SRRs. To begin with, we will assume that the CR is excited by a homogeneous external magnetic field $\mathbf{B}^{ext}=(B_x^{ext}, B_y^{ext}, B_z^{ext})$, and there is no external electric field. Then, the excitation vector is written as

$$\mathbf{F}_m = -j\omega A(B_x^{ext}, B_x^{ext}, B_y^{ext}, B_y^{ext}, B_z^{ext}, B_z^{ext}), \quad (13)$$

where A is the effective area of the SRR. By introducing Eq. (13) into Eq. (9), the current vector \mathbf{I} is calculated. Finally, the magnetic dipole components of the CR are obtained from $m_x=(I_1+I_2)A$, $m_y=(I_3+I_4)A$, and $m_z=(I_5+I_6)A$. The resulting expression for the magnetic polarizability tensor is

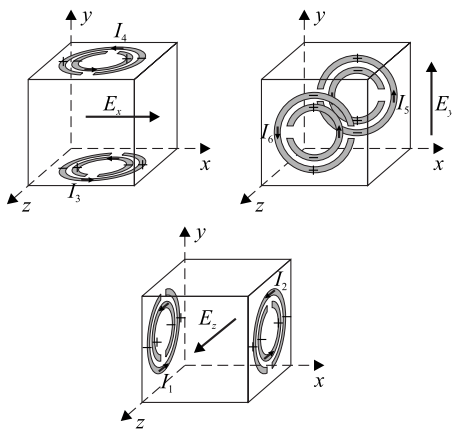


FIG. 5. Electric excitation of the cubic resonator made of Pendry's SRRs.

$$\boldsymbol{\alpha}^{mm} = -j\omega A^2 \frac{2}{3} \left[\frac{1}{Z_{11} + Z_{12} - Z_{13} - Z_{14}} \begin{pmatrix} 2 & -1 & 1 \\ -1 & 2 & 1 \\ 1 & 1 & 2 \end{pmatrix} + \frac{1}{Z_{11} + Z_{12} + 2Z_{13} + 2Z_{14}} \begin{pmatrix} 1 & 1 & -1 \\ 1 & 1 & -1 \\ -1 & -1 & 1 \end{pmatrix} \right]. \quad (14)$$

This magnetic polarizability tensor is anisotropic and exhibits two resonances, at those frequencies where $Z_{11} + Z_{12} - Z_{13} - Z_{14} \approx 0$ or $Z_{11} + Z_{12} + 2Z_{13} + 2Z_{14} \approx 0$. Only the even resonances of Table II appear in Eq. (14) because the excitation vector and the odd eigenvectors are orthogonal, i.e., $\mathbf{F}_m \cdot \mathbf{v}_i^{odd} = 0$ in Eq. (9). Just in the limit of no coupling between SRRs ($Z_{ij} = 0$ for $i \neq j$), both resonances converge to the single SRR resonance and $\boldsymbol{\alpha}_{mm}$ becomes a scalar, as mentioned in Refs. 14–16. However, it will be shown in the Sec. IV that this coupling cannot be neglected in most practical configurations.

Apart from the magnetic excitation studied above, it is well known that Pendry's SRR can be excited by an external electric field.^{5,6,40} Therefore, an electric response is also expected for this particular CR. The electric excitation of the rings on the cube is sketched in Fig. 5. The external electric field \mathbf{E}^{ext} can excite an SRR only if it has a nonvanishing component contained in the plane of the particle and orthogonal to the imaginary line passing through the slits of the rings.^{5,6,40} Therefore, only two SRRs are excited by each Cartesian component of \mathbf{E}^{ext} . Thus, for an external and homogeneous electric field of arbitrary direction, the excitation vector has the form

$$\mathbf{F}_e \propto (E_z^{ext}, -E_z^{ext}, -E_x^{ext}, E_x^{ext}, -E_y^{ext}, E_y^{ext}). \quad (15)$$

Taking into account the sign of the charges induced over the rings, it is clear that the electric dipole has to be proportional to

$$\mathbf{p} \propto \begin{pmatrix} I_3 - I_4 \\ I_5 - I_6 \\ I_2 - I_1 \end{pmatrix}. \quad (16)$$

The proportionality constants of Eq. (15) and (16) are given in the Appendix, Eqs. (A2) and (A9). Finally, from Eq. (A9) of the Appendix, we get the following analytical formula for the electric polarizability tensor:

$$\boldsymbol{\alpha}^{ee} = \frac{32d_{eff}^2}{3j\omega\pi^2} \left[\frac{1}{Z_{11} - Z_{12} - Z_{13} + Z_{14}} \begin{pmatrix} -2 & 1 & -1 \\ 1 & -2 & -1 \\ -1 & -1 & -2 \end{pmatrix} + \frac{1}{Z_{11} - Z_{12} + 2Z_{13} - 2Z_{14}} \begin{pmatrix} -1 & -1 & 1 \\ -1 & -1 & 1 \\ 1 & 1 & -1 \end{pmatrix} \right], \quad (17)$$

where d_{eff} is an effective distance between the metal strips on each SRR.^{5,6} Clearly, this electric polarizability tensor is anisotropic and exhibits two resonances, at those frequencies where $Z_{11} - Z_{12} - Z_{13} + Z_{14} \approx 0$ or $Z_{11} - Z_{12} + 2Z_{13} - 2Z_{14} \approx 0$. Only the odd resonances of Table II appear in Eq. (17) because the excitation vector and the even eigenvectors are orthogonal, i.e., $\mathbf{F}_e \cdot \mathbf{v}_i^{even} = 0$ in Eq. (9).

In summary, it has been shown that the coupling between the faces of the CR made of Pendry's SRRs shown in Fig. 1(a) splits the original resonance of a single SRR in four new resonances. Besides, both magnetic and electric polarizability tensors are anisotropic, as can be seen from Eqs. (14) and (17). Finally, it is worth mentioning that the even modes can also be called magnetic modes because they have a resonant magnetic moment and can be only excited by an external magnetic field but not by an external electric field. Similarly, the odd modes are electric modes because they present a resonant electric dipole, which can be only excited by an external electric field. The reported conclusions are quite relevant for our analysis because they show that a cubic arrangement of Pendry's SRRs will not be only anisotropic but it will also show several different resonances around the isolated SRR resonance, thus destroying any possibility of a single-resonance Lorentzian behavior of the metamaterial.

B. Analysis of an isotropic cube

It was already shown in Sec. II B that, in order to ensure an isotropic behavior, the CR has to be invariant at least under the tetrahedron symmetry group $T = \{\langle \mathbf{1}, \mathbf{4}_x, \mathbf{4}_y, \mathbf{4}_y \cdot \mathbf{4}_x \rangle\}$. The T -CR shown in Fig. 1(c), made of six NB-SRRs,^{8,13} is a good example of particle obeying this symmetry. By using the symmetry transformations and the rule [Eq. (5)], its impedance matrix can be significantly reduced to

$$\mathbf{Z} = \begin{bmatrix} Z_{11} & Z_{12} & Z_{13} & -Z_{13} & Z_{13} & -Z_{13} \\ Z_{12} & Z_{11} & -Z_{13} & Z_{13} & -Z_{13} & Z_{13} \\ Z_{13} & -Z_{13} & Z_{11} & Z_{12} & Z_{13} & -Z_{13} \\ -Z_{13} & Z_{13} & Z_{12} & Z_{11} & -Z_{13} & Z_{13} \\ Z_{13} & -Z_{13} & Z_{13} & -Z_{13} & Z_{11} & Z_{12} \\ -Z_{13} & Z_{13} & -Z_{13} & Z_{13} & Z_{12} & Z_{11} \end{bmatrix}, \quad (18)$$

where there are just three independent components. All eigenvalues and a complete set of orthonormal eigenvectors of

TABLE III. Eigenvalues and a complete set of orthonormal eigenvectors of the impedance matrix [Eq. (18)] corresponding to isotropic cubic resonators symmetric under the tetrahedron group $T=\{\langle \mathbf{1}, \mathbf{4}_x \cdot \mathbf{4}_y, \mathbf{4}_y \cdot \mathbf{4}_x \rangle\}$, as, for instance, the structure shown in Fig. 1(c).

	Eigenvalues z_i	Eigenvectors \mathbf{v}_i
Even modes	$Z_{11}+Z_{12}$	$\frac{1}{\sqrt{2}}(0,0,1,1,0,0)$
		$\frac{1}{\sqrt{2}}(0,0,0,0,1,1)$
		$\frac{1}{\sqrt{2}}(1,1,0,0,0,0)$
Odd modes	$Z_{11}-Z_{12}-2Z_{13}$	$\frac{1}{2\sqrt{3}}(1,-1,-2,2,1,-1)$
		$\frac{1}{2}(1,-1,0,0,-1,1)$
	$Z_{11}-Z_{12}+4Z_{13}$	$\frac{1}{\sqrt{6}}(-1,1,-1,1,-1,1)$

this matrix are shown in Table III. If we compare Tables III and II, we immediately find some similarities. In both cases, the eigenvectors can be classified into even and odd types, and the eigenvalues in Table III can be obtained from those of Table II by making $Z_{14}=-Z_{13}$. Furthermore, the odd and even subspaces are kept, and only the two subspaces of the even eigenvectors are unified into a single subspace due to the eigenvalue degeneration induced by the additional rotation symmetry $\mathbf{4}_x \cdot \mathbf{4}_y$.

Let us now analyze the resonances and polarizabilities of the T -CR by following the procedure developed in the previous subsection. By considering a homogeneous external magnetic excitation, the corresponding excitation vector [Eq. (13)] can only excite the even modes, thus leading to the isotropic magnetic polarizability tensor

$$\boldsymbol{\alpha}^{mm} = \frac{-2j\omega A^2}{Z_{11} + Z_{12}} \begin{bmatrix} 1 & 0 & 0 \\ 0 & 1 & 0 \\ 0 & 0 & 1 \end{bmatrix}, \quad (19)$$

which, in fact, corresponds to the substitution $Z_{14}=-Z_{13}$ in Eq. (14). The self-impedance in Eq. (19) is given by $Z_{11}=R+j\omega L+(j\omega C)^{-1}$, with R , L , and C being the resistance, self-inductance, and self-capacitance of a single NB-SRR.⁸ The mutual impedance in Eq. (19) can be approached as $Z_{12} \approx j\omega M_{12}$, where M_{12} is the mutual inductance between two NB-SRRs placed on opposite sides of the CR. This approximation is reasonable since the electric field is concentrated inside the gap of the NB-SRR, while the magnetic field created by a NB-SRR spreads out in space. Using these relations, the frequency of resonance of the CR can be cal-

culated as $\omega_{res} \approx [C(M_{12}+L)]^{-1/2}$, while the magnetic polarizability tensor takes the form

$$\boldsymbol{\alpha}^{mm} \approx \frac{2\omega^2 CA^2}{1 - \omega^2(L + M_{12})C + j\omega RC} \begin{bmatrix} 1 & 0 & 0 \\ 0 & 1 & 0 \\ 0 & 0 & 1 \end{bmatrix}. \quad (20)$$

This formula shows a Lorentzian-like magnetic response, similar to that of the single planar NB-SRR but isotropic in three dimensions.

With regard to the behavior of the considered CR under an external electric excitation, since the NB-SRRs cannot be excited by an external electric field,⁸ the present theory predicts the absence of any resonant response to this excitation (of course, the CR will exhibit a nonresonant electric polarizability due to the static electric moments induced on each ring, which is of no interest in the frame of the present discussion). However, experiments reported in Ref. 13 have shown that the considered CR exhibits a weak magnetoelectric coupling at the same resonant frequency, $\omega_{res}=[C(M_{12}+L)]^{-1/2}$, as in Eq. (20). Therefore, this phenomenon does not affect neither the isotropy nor the single-resonance behavior of the considered CR. Since the tetrahedron symmetry group, T , does not include the inversion transformation, this result is not forbidden for T -CRs. Although the origin of this effect will be qualitatively explained below in Sec. IV, it can be advanced that it is basically due to a second order electric interaction between SRRs, which is ignored in the equivalent circuit approximation developed in this section. Actually, the presence of this second order effect near the CR resonance shows how important the analysis of the spatial symmetries is in order to predict the behavior of metamaterial resonators: it seems that any effect not forbidden by symmetry will actually appear in practice, regardless of the equivalent circuit models. It is worth recalling here that this magnetoelectric coupling disappears if the T -CRs are arranged in an fcc lattice with $b=2a$, as explained at the end of Sec. II B.

IV. EXPERIMENTS

For the experimental verification of the theory developed in the previous sections, some anisotropic and isotropic CRs were manufactured. Each CR was inserted into a standard WR430 waveguide, as shown in Fig. 6. The testing procedure starts from the fact that the particle is isotropic if their polarizability tensors are invariant by any rotation. Therefore, all CRs were subjected to several rotations and the transmission coefficient through the waveguide was measured using a network analyzer HP-8510. If the measured CR were isotropic, then the measured transmission coefficient would remain invariant after rotations.

Namely, two anisotropic cubes made of Pendry's SRRs and omega particles and two isotropic cubes made of C_2 -SRRs (actually NB-SRRs⁸) and C_4 -SRRs (see insets in Fig. 7) were implemented. All SRRs were etched on Arlon 250-LX substrate with dielectric constant $\epsilon_r=2.43$, loss tangent $\tan \delta < 0.002$, and thickness $t=0.49$ mm. In order to check the similarity between the SRRs belonging to the same CR, their resonance frequencies were measured by placing

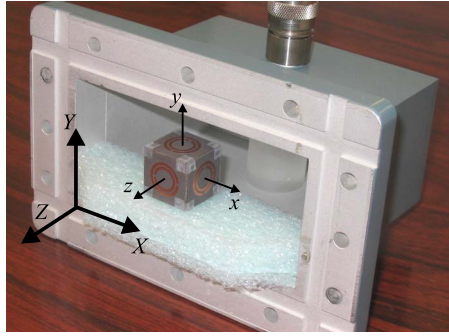


FIG. 6. (Color online) Experimental setup for checking the isotropy of cubic resonators. In the illustration, a cubic resonator made of Pendry's SRR is placed inside a pair of standard waveguide-coaxial transitions WR430 connected to a network analyzer HP-8510-B. The transversal dimensions of the waveguide are $109 \times 55 \text{ mm}^2$ and its frequency range is 1.7–2.6 GHz. The cube is held by a piece of electromagnetically inert foam at an arbitrary orientation.

each one in the E plane of the waveguide, obtaining the following values: $f_0^{\text{Pendry's SRR}} = (2.321 \pm 0.002)$ GHz, $f_0^{\Omega} = (2.216 \pm 0.002)$ GHz, $f_0^{\text{C4-SRR}} = (2.399 \pm 0.001)$ GHz, and $f_0^{\text{NB-SRR}} = (2.385 \pm 0.002)$ GHz. These results show that significant deviations from these values (of more than 0.002 GHz) in the measured resonances of the transmission coefficients for the CRs must be interpreted as a resonance splitting due to SRR couplings, and not due to fabrication imprecision. The SRRs were assembled over a cube of isotropic dielectric (ROHACELL 71 HF, $\epsilon_r = 1.07$, $\tan \delta < 0.0002$) of size $2 \times 2 \times 2 \text{ cm}^3$. More details on the preparation of the experiments are given in Ref. 41.

A. Anisotropic cubes

First, the CRs not satisfying the necessary spatial symmetries for isotropy were tested. Figure 7(a) shows the transmission coefficient through the waveguide loaded with the CR made of Pendry's SRRs. Two observations are apparent: there are three major resonance peaks and none of them stays invariant under rotations of the cube. Therefore, this CR is anisotropic, as theoretically predicted by the symmetry theory in Sec. II B. However, the circuit model developed in Sec. III A predicts the presence of four different resonances, but not three, as can be observed in Fig. 7(a). Although this fourth resonance is not clearly visible in Fig. 7(a), the dip at the lowest frequency is split into two dips for the other different orientation shown in Ref. 42, thus recovering the agreement with the theory. Furthermore, in Ref. 42, the nature of each resonance is identified as electric or magnetic.

The cube composed of omega particles was also experimentally tested. This cube has symmetry properties identical as the cube made of Pendry's SRR, i.e., it is invariant under the inversion and the rotation $\mathbf{4}_y \cdot \mathbf{4}_x$. The transmission coefficient for this measurement is depicted in Fig. 7(b), where similar results as for the SRR cube can be observed. Namely, the original resonance of a single omega particle now appears split in several resonances and the transmission coeffi-

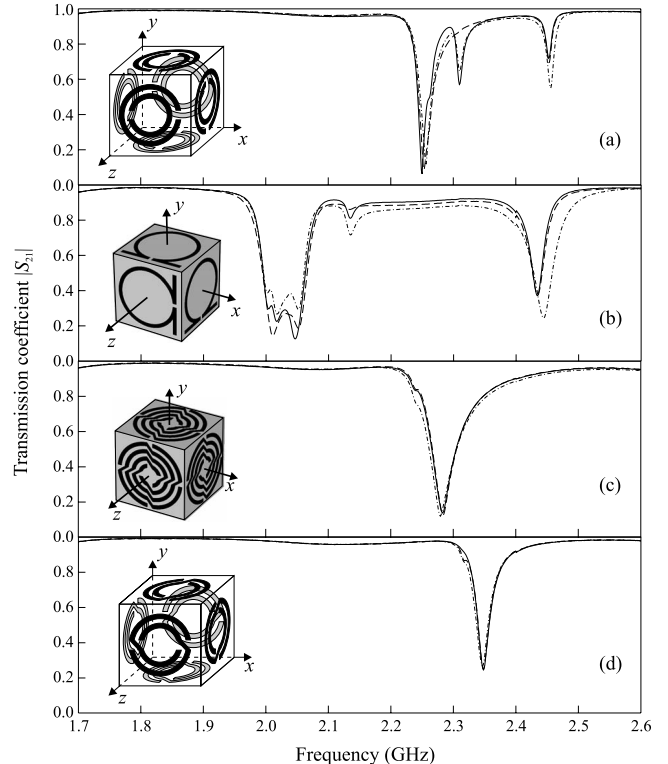


FIG. 7. Transmission coefficient ($|S_{21}|$) through a waveguide containing a cubic resonator made of (a) Pendry's SRRs, (b) Omega particles, (c) C_4 -SRRs, or (d) C_2 -SRRs (or NB-SRR). Solid line: the particle is oriented with its axes (x, y, z) parallel to the waveguide axes (X, Y, Z) shown in Fig. 6. Dashed line: the first orientation is rotated by 45° along the Y axis. Dash-dot line: the first orientation is rotated by 45° along the Z axis and 45° along the Y axis. The size of all cubes is $2 \times 2 \times 2 \text{ cm}^3$. Dimensions of Pendry's SRRs: external radius $r_{ext} = 7 \text{ mm}$, width of the strip $w = 1.25 \text{ mm}$, distance between strips $d = 0.5 \text{ mm}$, and size of split gap $g = 1 \text{ mm}$. Dimensions of Ω : $r_{ext} = 8.5 \text{ mm}$, $w = 1 \text{ mm}$, $g = 1 \text{ mm}$, and the length of "legs" $l = 8 \text{ mm}$. Dimensions of C_4 -SRR: $r_{ext} = 9.25 \text{ mm}$, $w = 1.25 \text{ mm}$, $d = 0.5 \text{ mm}$, and $g = 1.5 \text{ mm}$. Dimensions of C_2 -SRR: external radius $r_{ext} = 7 \text{ mm}$, width of the strip $w = 1.25 \text{ mm}$, distance between strips $d = 0.5 \text{ mm}$, and size of split gap $g = 1 \text{ mm}$.

cient changes for different orientations. However, the number of resonance dips in Fig. 7(b) is 5 instead of 4, as previously predicted in Sec. III A. This failure of the model can be attributed to a strong electric coupling between the legs of two neighbors. In fact, it can be expected from the CR depicted in Fig. 7(b) that the electric field between legs of two omega particles on adjacent sides of the CR is comparable to the internal electric field in each omega particle. Thus, the CR should be seen as an inseparable particle instead of six RLC circuits, as assumed in Sec. III.

An important result of the reported measurements is that the relative frequency deviations between the different resonances of the CRs made of Pendry's SRRs and omega particles (10% or more with regard to the central frequency) are of the same order that the bandwidths reported for most SRR or omega based negative- μ metamaterials. Therefore, as advanced in Sec. III, it can be guessed that any metamaterial made from such configurations will show multiple reso-

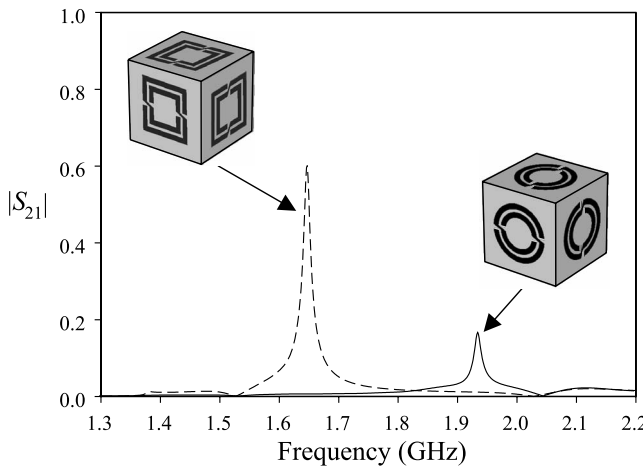


FIG. 8. Simulated transmission coefficient ($|S_{21}|$) through the cross polarization waveguide setup filled by T-CRs made of circular (solid line) and square NB-SRRs (dashed line). Dimensions of the circular NB-SRR: external diameter $2r_{ext}=20$ mm, width of the strip $w=2$ mm, distance between strips $d=1$ mm, and size of split gap $g=1.6$ mm. The square NB-SRRs have similar dimensions and the same external perimeter. Cube edge was 24 mm long.

nances inside the expected negative- μ frequency band, thus destroying any single-resonance Lorentzian behavior.

B. Isotropic cubes

In order to show the usefulness of spatial symmetries to provide isotropic resonators, the cubes made of C_4 -SRRs and C_2 -SRRs [see insets in Figs. 7(c) and 7(d)], satisfying the octahedron group O and the tetrahedron group T , respectively, have been tested. As shown in Sec. II B, both cubes are symmetric enough to be isotropic. The transmission coefficients for these CRs are shown in Figs. 7(c) and 7(d). It can be observed that the transmission does not depend on their orientations, thus demonstrating their isotropy. Besides, it can be seen that only one peak appear in both measurements, as predicted in Sec. III B. It is worth noting that a similar result will be obtained for any CR satisfying any one of the five cubic symmetry point groups (T , T_h , T_d , O , and O_h).

The cubes analyzed in this section have no inversion symmetry and, as mentioned at the end of Sec. III, they could exhibit a bi-isotropic behavior. However, from the experimental curves, it is impossible to see whether the analyzed CRs are bi-isotropic or not. To examine this possibility, electromagnetic simulations of a square waveguide loaded with T-CRs were made. The input port was fed by the TE_{10} mode, while the TE_{01} mode with orthogonal polarization was measured on the output port. The resulting cross-polarization transmission coefficient is shown in Fig. 8. The nonzero transmission means that the incident electric field can excite not only a parallel electric dipole but also a parallel magnetic dipole. From reciprocity, it is also clear that an incident magnetic field can excite both magnetic and electric dipoles parallel to the exciting field. This result clearly shows the bi-isotropic behavior of the C_2 -SRR cube. In order to show that

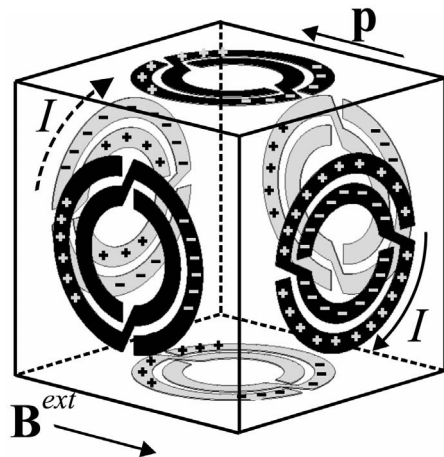


FIG. 9. Illustration of the bi-isotropic behavior of a T -CR made of NB-SRRs driven by an external magnetic field.

the bi-isotropy can be avoided by including the inversion symmetry in the configuration, a similar simulation was carried out for the T_h -CR shown in Fig. 1(d), already proposed in,¹³ which possesses an inversion symmetry. The transmission coefficient, not depicted here, was almost zero and of the same order as the transmission through the waveguide without any resonator, thus showing that this last configuration is not bi-isotropic.

As already reported, the bi-isotropy of the T -CR cannot be explained by the circuit model proposed in Sec. III. The explanation of this effect seems to rely on the electric coupling between the edges of two SRR on adjacent faces of the cube. To understand this in a qualitative way, let us assume that the cube is driven by an external magnetic field feeding only two resonators in the cube, as shown in Fig. 9. This figure also depicts the current and corresponding charges induced by the external field on each NB-SRR. Due to the inversion symmetry of the NB-SRR, the electric dipole generated by the excited resonators is zero.⁸ However, Fig. 9 also shows how the induced resonant charges polarize the other (not excited) rings. These are polarized in such a way that the CR acquires a net electric dipole, as sketched in the figure. This dipole does not excite an extra net current on the NB-SRR since the polarization charge symmetrically flows on both halves of the resonator. Therefore, this effect is not taken into account by the circuit model reported in Sec. III. However, it introduces a nonzero magnetoelectric polarizability that cannot be extracted from that model. According to the above explanation, it is expected that magnetoelectric coupling will increase if the electric coupling between the edges of neighboring resonators grows. To check this hypothesis, the cross-polarized transmission was also computed for square rings (see dashed line in Fig. 8). The enhancement of the magnetoelectric coupling can be clearly observed in this case.

At the end of Sec. II, it was mentioned that this bi-isotropic behavior would disappear in an fcc cubic lattice with $b=2a$ (see Fig. 3). In that section, this behavior was predicted on the basis of the particular symmetry of this specific lattice. The illustration in Fig. 9 of the bi-isotropy of an isolated CR made of six identical NB-SRRs also provides a qualitative physical interpretation of such result: if additional

SRRs were added to Fig. 9 in order to make an fcc cubic lattice, it becomes apparent that the induced charges on the nonresonant additional SRRs will cancel the total electric dipole shown in the figure.

V. CONCLUSIONS

A systematic approach to the design of isotropic magnetic metamaterials by using isotropic cubic magnetic resonators in a cubic lattice has been developed. For this purpose, cubic magnetic resonators obeying some cubic point groups of symmetry (T , T_d , T_h , O , or O_h) placed in cubic Bravais' lattice (sc, bcc, or fcc) were analyzed. Special care has been taken in the study of the symmetry of the constitutive elements (also called cubic resonators or CRs). For practical reasons, CRs made of six modified SRRs assembled over the surface of a cube were considered. The connection between the orientations of these SRRs over the cube and the cubic point groups of symmetry has been analyzed. Starting from this analysis, some particular examples of anisotropic and isotropic CRs were analyzed, manufactured, and measured. It was analytically and experimentally shown that the lack of the necessary symmetry leads to an anisotropic response. In experiments, the transmission through a waveguide loaded with the manufactured CRs was measured, getting a strong dependence of this parameter on the orientation for anisotropic CRs, while the transmission was invariant with respect to the orientation for isotropic CRs. Furthermore, the splitting of the isolated SRR resonances into several resonances was observed in anisotropic CRs. This effect is absent in isotropic CRs, which always show a single resonance. Most of these effects were theoretically explained by using an equivalent circuit model, which takes into account the electromagnetic couplings between the SRRs making the analyzed CRs.

From a practical standpoint, we have found that using some low symmetry CRs, pertaining to the tetrahedral group T or T_h , placed in a cubic Bravais lattice is enough to provide isotropy in three dimensions. Using CRs with lower symmetry results in an anisotropic behavior, even if the dipole representation of the SRRs suggests an isotropic behavior. In general, using cubic resonators pertaining to a symmetry group which does not include inversion (such as the symmetry group T) produces a bi-isotropic behavior, even if the isolated SRRs making the metamaterial do not present magnetoelectric coupling. However, this bi-isotropy can be avoided by a proper choice of the lattice. In particular, it has been shown that cubic resonators pertaining to the aforementioned T group placed in an fcc lattice with the appropriate periodicity can produce a purely magnetic isotropic behavior.

We hope that the reported results will pave the way to the design of isotropic three-dimensional periodic metamaterials with a resonant magnetic response, including negative permeability and left-handed metamaterials.

ACKNOWLEDGMENTS

This work has been supported by the Spanish Ministry of Education and Science under Project No. TEC2004-04249-

C02-02, by the Spanish Junta de Andalucía under Project No. P06-TIC-01368, and by the Grant Agency of Czech Republic under Project No. 102/03/0449. Authors also thank Esperanza Rubio for manufacturing the resonators used in the experiments.

APPENDIX: ELECTRIC EXCITATION OF THE CUBIC RESONATOR MADE OF PENDRY'S SPLIT RING RESONATOR

Let us assume a single SRR placed in the xy plane with its two slits along the x axis. The electromotive force can be approximated by averaging the path integral of the external electric field through the gap along the circumference of the particle, so that

$$\begin{aligned} \text{emf} = \langle \mathbf{E}^{\text{ext}} \cdot \mathbf{d}_{\text{eff}}(\varphi) \rangle &= 2E_y^{\text{ext}} d_{\text{eff}} \frac{1}{\pi} \int_0^\pi \cos(\varphi - \pi/2) d\varphi \\ &= \frac{4}{\pi} d_{\text{eff}} E_y^{\text{ext}}. \end{aligned} \quad (\text{A1})$$

It is worth noting that the two halves of the SRR are polarized in the same direction,^{5,6} so that it justifies the factor 2 in front of the integral and its integration domain $(0, \pi)$. Now, let us generalize the electromotive force of Eq. (A1) to get the “excitation vector” for the CR made of Pendry's SRRs shown in Fig. 1(a). Taking into account the sketch of the excitation shown in Fig. 5, it is easy to get the following electric excitation vector:

$$\mathbf{F}_e = \frac{4}{\pi} d_{\text{eff}} (E_z^{\text{ext}}, -E_z^{\text{ext}}, -E_x^{\text{ext}}, E_x^{\text{ext}}, -E_y^{\text{ext}}, E_y^{\text{ext}}). \quad (\text{A2})$$

In what follows, for simplicity, the superscript ext will be avoided. By introducing Eq. (A2) in Eq. (9), we get the associated currents

$$\begin{aligned} \begin{pmatrix} I_1 \\ I_2 \\ I_3 \\ I_4 \\ I_5 \\ I_6 \end{pmatrix} &= \frac{\frac{4}{3\pi} d_{\text{eff}}}{Z_{11} - Z_{12} - Z_{13} + Z_{14}} \begin{pmatrix} E_x + E_y + 2E_z \\ -E_x - E_y - 2E_z \\ -2E_x + E_y - E_z \\ 2E_x - E_y + E_z \\ E_x - 2E_y - E_z \\ -E_x + 2E_y + E_z \end{pmatrix} \\ &+ \frac{\frac{4}{3\pi} d_{\text{eff}}}{Z_{11} - Z_{12} + 2Z_{13} - 2Z_{14}} \begin{pmatrix} -E_x - E_y + E_z \\ E_x + E_y - E_z \\ -E_x - E_y + E_z \\ E_x + E_y - E_z \\ -E_x - E_y + E_z \\ E_x + E_y - E_z \end{pmatrix}. \end{aligned} \quad (\text{A3})$$

The electric dipole for a single SRR can be expressed in terms of a linear charge density λ as^{5,6}

$$p_y = 2\lambda r_0 d_{eff} \int_0^\pi \cos(\varphi - \pi/2) d\varphi = 4\lambda r_0 d_{eff}, \quad (\text{A4})$$

where d_{eff} is an effective distance between the two metallic strips forming the SRR. The charge density on the inner, I_i , and outer rings, I_o , of the SRR can be calculated by means of the charge conservation law as follows:

$$\frac{dI_{i,o}}{d\theta} = j\omega r \lambda_{i,o} \Rightarrow \lambda_{i,o} = \frac{1}{j\omega r} \frac{dI_{i,o}}{d\theta}. \quad (\text{A5})$$

Since the SRR size is much smaller than one wavelength, we can suppose a linear variation of $I_{i,o}$ respect to the angle ϕ , taking its maximum value, I , at the center of the metal strip and zero at its ends, as in Refs. 4 and 5. Then,

$$|\lambda| = \frac{1}{j\omega r} \frac{|I|}{\pi}. \quad (\text{A6})$$

Although I_i and I_o are not uniform through ϕ , the sum of both, $I_i + I_o$, is approximately constant and equal to the current I , which is actually the effective current associated with the averaged loop. By Eqs. (A4) and (A6), we obtain

$$|p_y| = \frac{4d_{eff}}{j\omega\pi} |I|. \quad (\text{A7})$$

Now, we can calculate the total electric moment of the SRR cube by adding the six moments. By considering Eq. (A7) and taking into account the signs of the charges shown in Fig. 5, we obtain the electric dipole

$$\mathbf{p} = \frac{4d_{eff}}{j\omega\pi} \begin{pmatrix} I_3 - I_4 \\ I_5 - I_6 \\ I_2 - I_1 \end{pmatrix}. \quad (\text{A8})$$

Finally, by substituting the currents of Eq. (A3) into Eq. (A8), we get the electric dipole in terms of the components of the external electric field,

$$\mathbf{p} = \frac{32d_{eff}^2}{3j\omega\pi^2} \left[\frac{1}{Z_{11} - Z_{12} - Z_{13} + Z_{14}} \begin{pmatrix} -2E_x + E_y - E_z \\ E_x - 2E_y - E_z \\ -E_x - E_y - 2E_z \end{pmatrix} \right. \\ \left. + \frac{1}{Z_{11} - Z_{12} + 2Z_{13} - 2Z_{14}} \begin{pmatrix} -E_x - E_y + E_z \\ -E_x - E_y + E_z \\ E_x + E_y - E_z \end{pmatrix} \right]. \quad (\text{A9})$$

*juan_dbd@us.es

†l_jelinek@us.es

‡marques@us.es

¹V. G. Veselago, Sov. Phys. Usp. **10**, 509 (1968).

²D. R. Smith, W. J. Padilla, D. C. Vier, S. C. Nemat-Nasser, and S. Schultz, Phys. Rev. Lett. **84**, 4184 (2000).

³J. B. Pendry, A. J. Holden, D. J. Robbins, and W. J. Stewart, IEEE Trans. Microwave Theory Tech. **47**, 2075 (1999).

⁴W. Rotman, IRE Trans. Antennas Propag. **10**, 82 (1962).

⁵R. Marqués, F. Medina, and R. Rafii-El-Idrissi, Phys. Rev. B **65**, 144440 (2002).

⁶R. Marqués, F. Mesa, J. Martel, and F. Medina, IEEE Trans. Antennas Propag. **51**, 2572 (2003).

⁷J. D. Baena, R. Marqués, F. Medina, and J. Martel, Phys. Rev. B **69**, 014402 (2004).

⁸J. D. Baena, J. Bonache, F. Martín, R. Marqués, F. Falcone, T. Lopetegui, M. A. G. Laso, J. García-García, I. Gil, and M. Flores, IEEE Trans. Microwave Theory Tech. **53**, 1451 (2005).

⁹J. B. Pendry, Phys. Rev. Lett. **85**, 3966 (2000).

¹⁰A. L. Pokrovsky and A. L. Efros, Phys. Rev. Lett. **89**, 093901 (2002).

¹¹R. Marqués and D. R. Smith, Phys. Rev. Lett. **92**, 059401 (2004).

¹²P. Gay-Balmaz and O. J. F. Martin, Appl. Phys. Lett. **81**, 939 (2002).

¹³J. D. Baena, L. Jelinek, R. Marqués, and J. Zehentner, Appl. Phys. Lett. **88**, 134108 (2006).

¹⁴C. R. Simovski and S. He, Phys. Lett. A **311**, 254 (2003).

¹⁵C. R. Simovski and B. Sauviac, Radio Sci. **39**, RS2014 (2004).

¹⁶E. Verney, B. Sauviac, and C. R. Simovski, Phys. Lett. A **331**, 244 (2004).

¹⁷L. Jelinek, J. Zehentner, J. D. Baena, and R. Marqués, Proceedings of IEEE MELECON 2006, Benalmádena (Málaga), Spain,

16–19 May 2006, p. 250.

¹⁸Th. Koschny, L. Zhang, and C. M. Soukoulis, Phys. Rev. B **71**, 121103(R) (2005).

¹⁹W. J. Padilla, Opt. Express **15**, 1639 (2007).

²⁰C. L. Holloway, E. F. Kuester, J. Baker-Jarvis, and P. A. Kabos, IEEE Trans. Antennas Propag. **51**, 2596 (2003).

²¹I. Vendik, O. Vendik, I. Kolmakov, and M. Odit, Opto-Electron. Rev. **14**, 179 (2006).

²²G. V. Eleftheriades, A. K. Iyer, and P. C. Kremer, IEEE Trans. Microwave Theory Tech. **50**, 2702 (2002).

²³W. J. R. Hoefer, P. P. M. So, D. Thompson, and M. Tentzeris, IEEE International Microwave Symposium Digest, Long Beach, CA, June 2005, pp. 313–316.

²⁴A. Grbic and G. V. Eleftheriades, J. Appl. Phys. **98**, 043106 (2005).

²⁵P. Alitalo, S. Maslovski, and S. Tretyakov, J. Appl. Phys. **99**, 064912 (2006).

²⁶P. Alitalo, S. Maslovski, and S. Tretyakov, J. Appl. Phys. **99**, 124910 (2006).

²⁷T. J. Yen, W. J. Padilla, N. Fang, D. C. Vier, D. R. Smith, J. B. Pendry, D. N. Basov, and X. Zhang, Science **303**, 1494 (2004).

²⁸S. Linden, C. Enkrich, M. Wegener, J. Zhou, T. Koschny, and C. M. Soukoulis, Science **306**, 1351 (2004).

²⁹S. A. Tretyakov, A. Sihvola, and L. Jylhä, Photonics Nanostruct. Fundam. Appl. **3**, 107 (2005).

³⁰R. Marqués, L. Jelinek, and F. Mesa, Microwave Opt. Technol. Lett. **49**, 2606 (2007).

³¹I. V. Lindell, A. Sihvola, S. A. Tretyakov, and A. J. Viitanen, *Electromagnetic Waves in Chiral and Bi-Isotropic Media* (Artech House, Norwood, MA, 1994).

³²N. W. Ashcroft and N. D. Mermin, *Solid State Physics* (Holt, Rinehart and Winston, Philadelphia, 1976).

- ³³J. F. Nye, *Physical Properties of Crystals: Their Representation by Tensors and Matrices* (Clarendon, Oxford, 1993).
- ³⁴A. Sihvola, *Electromagnetic Mixing Formulas and Applications* (The Institution of Electrical Engineers, London, 1999).
- ³⁵M. M. I. Saadoun and N. Engheta, *Microwave Opt. Technol. Lett.* **5**, 184 (1992).
- ³⁶J. García-García, F. Martín, J. D. Baena, R. Marqués, and L. Jelinek, *J. Appl. Phys.* **98**, 033103 (2005).
- ³⁷S. O'Brien and J. B. Pendry, *J. Phys.: Condens. Matter* **14**, 6383 (2002).
- ³⁸C. R. Simovski, S. A. Tretyakov, A. A. Sochava, B. Sauviac, F. Mariotte, and T. G. Kharina, *J. Electromagn. Waves Appl.* **11**, 1509 (1997).
- ³⁹R. F. Harrington, *Time-Harmonic Electromagnetic Fields* (McGraw-Hill, New York, 1961), p. 119.
- ⁴⁰P. Gay-Balmaz and O. J. F. Martin, *J. Appl. Phys.* **92**, 2929 (2002).
- ⁴¹See EPAPS Document No. E-PRBMDO-76-032744 for additional information about the “Preparation of experiments.” For more information on EPAPS, see <http://www.aip.org/pubservs/epaps.html>.
- ⁴²See EPAPS Document No. E-PRBMDO-76-032744 for additional information about the “Identification of the resonances of the Pendry’s SRR-CR.” For more information on EPAPS, see <http://www.aip.org/pubservs/epaps.html>.